Advances in Geological and Geotechnical Engineering Research
https://ojs.bilpublishing.com/index.php/agger

ARTICLE

A Typical Sublithospheric Mantle beneath the Tello Region, SE-Ngaoundéré (Cameroon Line)

Nguihdama Dagwai[1*] **Kamgang Pierre**[2] **Mbowou Gbambié Isaac Bertrand**[3] **Chazot Gilles**[4] **Ngounouno Ismaïla**[3]

1. École Normale Supérieure, Université de Maroua, Cameroun
2. Département des sciences de la Terre, Faculté des Sciences, Université de Yaoundé I, Yaoundé, Cameroun
3. École de Géologie et d'Exploitation Minière (EGEM), Département de Mines et de la Géologie, Université de Ngaoundéré, Meiganga, Cameroun
4. Université Européenne de Bretagne, Brest, France

ARTICLE INFO

Article history
Received: 29 March 2022
Revised: 29 April 2022
Accepted: 05 May 2022
Published Online: 12 May 2022

Keywords:
Spinel-Lherzolite xenoliths
Protogranular
Sublithospheric mantle
Tello
Cameroon line

ABSTRACT

Peridotite xenoliths, raised to the surface by alkaline basalts or kimberlites, provide us direct information on the processes and composition of the upper mantle. They are the major source of information on the state of stress, pressure and temperature in the deep mantle. They are thus a source of petrological and geochemical information that is generally not available on the Earth's surface. Fresh spinel-lherzolite xenoliths exhibit a protogranular components of the Tello volcano. The Tello is the continental sector of the Cameroon Line, located in the South East of the town of Ngaoundéré at 75 km approximately between (N7° 13', N7° 14') and (E13° 40' and E13° 60'). Minerals' composition of the xenoliths is ~64% olivine, ~24% orthopyroxene, ~11% clinopyroxene and ~1% spinel. Significant variation in (Cr/Cr + Al) of the system shows the reciprocal nature of the spinel solution.The Tello spinel lherzolites show internal chemical homogeneity and represent a normal upper mantle. Their mineral chemistries suggest equilibrium condition of 830° - 925° and 1.4 GPa-2.3 GPa. These data suggest that there is good correlation bracket between increasing activity of Al_2O_3 and decreasing of practionning of TiO_2 into spinel. The Al^{IV} and Al^{VI} contents vary by 0.05-0.2 and 0.03-0.2 respectively. The majority of samples caracterise the lithospheric mantle.

1. Introduction

The "Cameroon Volcanic Line" (LVC) is an active tectono-magmatic alignment oriented N30°E, from the island of Pagalù to Lake Chad [1]. This line is a major geological structure in Central Africa whose impor-

---

*Corresponding Author:
Nguihdama Dagwai,
École Normale Supérieure, Université de Maroua, Cameroun;
Email: da_nguihdama76@yahoo.fr

DOI: https://doi.org/10.30564/agger.v4i2.4580

tance can be compared to the "Rift-Valley system" of East Africa [2]. This chain of intraplate volcanoes covers more than 1600 km long [3] by 100 km wide [4]. It thus offers the particularity of being one of the few magmatic entities built at the same time in the oceanic and continental domains [1]. Structurally, field observations, interpretation of aerial photographs [4] have made it possible to identify major fracture directions or major lineaments among which one has the direction N70°E or direction Adamaoua. The geomorphology of the Tello is characterized by the presence of volcanic material ejected from the crater just at the external limits. The cones are generally open on the sides. The specific case of the fall is open on the SSW side marked by the presence of a flaring of the crater setting up a laccolite-shaped cave (Figure 1). The cave is generally marked along the sides by the presence of mantle xenoliths well formed and well encrusted in the basalts. Tello xenolites are fragments of mantellic rocks carried by the magma to the surface during the volcanic eruption.

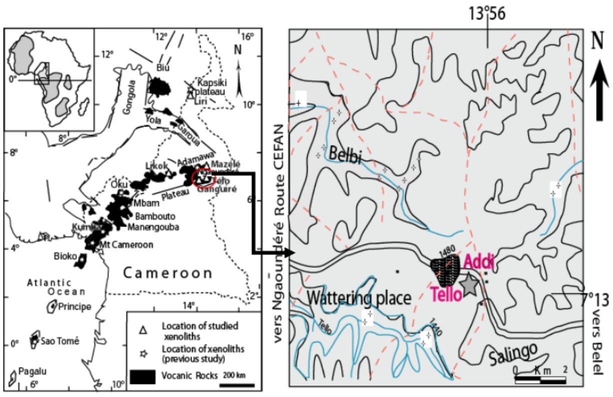

Figure 1. Location of the ultramafic xenoliths of the study area from the Hosséré Addi (Tello) and from the other sectors of the Cameroon Volcanic Line and the Adamawa Plateau

2. Geological Setting

The structures of the Adamaoua plateau are locally covered with more or less altered volcanic formations. Observations of these structures from aerial photographs [5] on gneissic series and veins of volcanic rocks have made it possible to highlight other dominant directions on the EW plateau in its West part and N170°E in its East part. All the magmatic occurrences were set up in the pan-African substratum rich in calcalkaline granitoids and sometimes covered by volcano-sedimentary formations of Paleozoic age of the Mangbéi type or by Cretaceous sedimentary formations of Mamfé and Bénoué [6]. One of the morphological features of the region is represented by the Ngaoundere cliff (Mbé), which is a fault mirror 600 m high, where several directions interfere. The intense fracturing of the rocks in the Ngaoundere area is attributed to a NW-SE direction compression probably of Cretaceous age [5], and followed by other phases of creative deformations of the current reliefs. Tectonic movements responsible for the first Adamaoua uprising took place in Cenomania [6]. The region was then subjected to tectonic compression forces that resulted in significant setbacks, including the South Adamaoua dextre, which gives its current shape, the horst and grabens model, due to fractures and compressions [7].

3. Analytical Methods

The mineral phases of the Tello xenolites were carried out under the conditions on the Cameca SX 100 microprobe of the West Microsonde service in Brest (France). The test conditions were 15 kV for the acceleration voltage, for currents of 10 nA or 20 nA depending on the resistance of the minerals to the electron beam. The samples analysed are thin strips of rocks of different types (xenoliths) and the analyses are carried out on polished sections in the European University of Bretagne, Brest, France at service microsonde west. Before each run, the samples are carbon metallized. Then a very fine electron incident beam comes into contact with the sample. Radiation is then analyzed by spectrometers that each explores a range of precise wavelengths. It is possible to make a quantitative analysis of a given element if the spectrometer is fixed at the corresponding characteristic wavelength.

4. Results

4.1 Petrography

At Tello, the cave is generally marked along the flanks by the presence of well-formed mantle xenoliths, well embedded in the basalts. The xenoliths size is varying between ten and thirty centimeters along the sides of the caves (Figure 2a).

Tello (To) spinel peridotites have a coarse grained texture. Kernels with curvilinear boundaries are disseminated in mesostasis. The texture is protogranular [8]. The silicates of xenoliths are composed of orthopyroxene, clinopyroxene, olivine, and spinel. The microscopic observation of Tello's thin blade shows large minerals (3 mm to 4 mm) and gives the blade a granoblastic texture. The minerals observed are orthopyroxen (Opx), clinopyroxen (Cpx), spinel (Sp) and olivine (Ol) (Figure 2b).

4.2 Mineral Chemistry

4.2.1 Olivine

Olivine has a high forsterite content (91 < Fo < 92). The concentration by weight of NiO is between 0.3% and

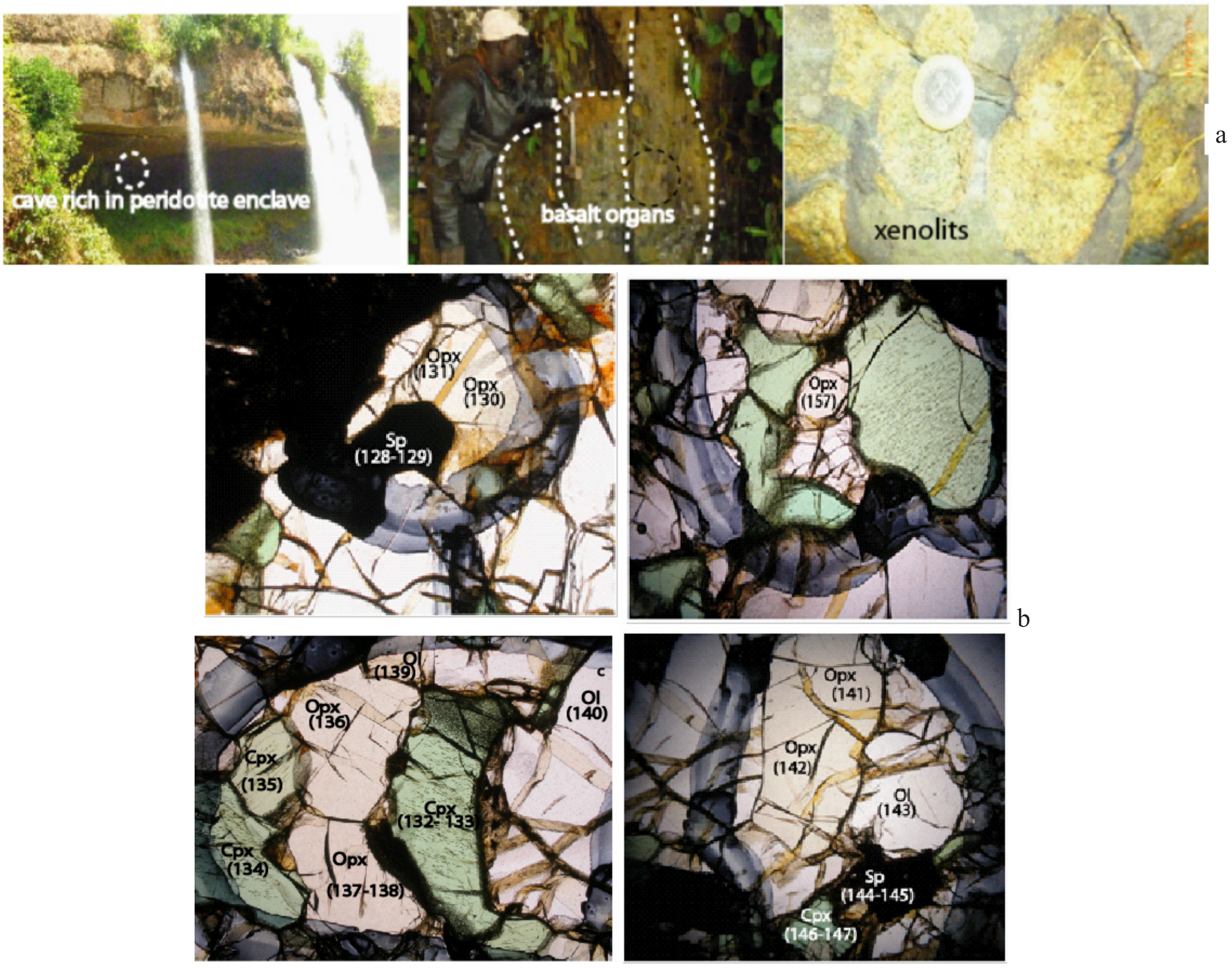

Figure 2. Thin sections of peridotites observed with optical microscope under crossed nicols. (cpx = clinopyroxene, ol= olivine, opx =orthopyroxene and sp = spinel, abbreviation [9] (a) and macro views of the xenoliths (b).

0.5% (Table 1). There is a positive correlation between NiO and the forsterite content of olivine.

Table 1. Olivine compositions (wt% and a.p.f.u. on the basis 4 oygens)

data/Point	139 /1.	143 /1.	140 /1.	162 /1.
SiO_2	41.08	41.18	41.23	40.95
TiO_2	0.00	0.03	0.01	0.00
Al_2O_3	0.02	0.04	0.01	0.02
Cr_2O_3	0.00	0.00	0.01	0.00
FeO	7.87	7.90	7.74	7.73
MnO	0.15	0.11	0.16	0.12
MgO	51.34	50.75	50.82	51.35
CaO	0.04	0.13	0.05	0.02
NiO	0.44	0.35	0.41	0.40
Na_2O	0.00	0.00	0.00	0.00
P_2O_5	0.00	0.05	0.00	0.00
Total	100.93	100.54	100.44	100.58
Si	0.991	0.997	0.998	0.990
Fe^{2+}	0.159	0.160	0.157	0.156
Mn	0.003	0.002	0.003	0.002
Mg	1.846	1.831	1.834	1.852
Ca	0.001	0.003	0.001	0.001
Ni	0.009	0.007	0.008	0.008
Fo	91.95	91.87	91.98	92.10
Fa	8.05	8.13	8.02	7.90

4.2.2 Clinopyroxene

The compositions of the clinopyroxenes (En_{48-49} $Wo_{47-48}Fs_{2-3}$) of Tello (b) fall into the field of diopside. Their TiO_2 levels are less than 0.55%, and those of Al_2O_3 vary between 5.88%-6.27%. Clinopyroxene is characterized by a high value in Mg# 98%, that of orthopyroxene and olivine. Their $Al^{VI}I/Al^{IV}$ ratio varies between 1.11 and 1.92 (Figure 3) [10]. The TiO_2 contents range from 0.17 wt% to 0.30 wt% and those of Al_2O_3 from 4.29 wt% to 4.49

wt% (Table 2). These diopside crystals are Cr-rich with the values of Cr# [Cr# = 100 × atomic Cr/(Cr + Al)] (17.29 - 19.91) typical of Cr-diopside [11]. The clinopyroxene is characterized by Mg# [Mg# = 100 × atomic Mg/(Mg + Fe^{2+})] values of 93 - 94, higher than those of coexisting orthopyroxene (see below) and olivine. The values of Al^{VI}/Al^{IV} ratio range between 1.1 and 1.3 for the Cr-diopside crystals from Hosséré Addi xenoliths.

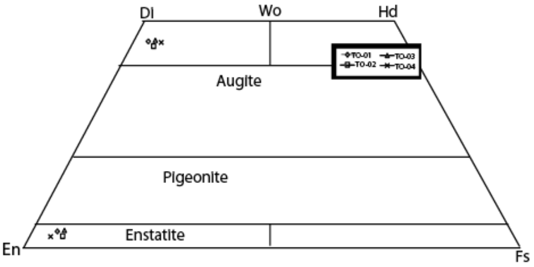

Figure 3. Compositions of the pyroxenes analyzed in the Spinel-Xenoliths of Tello [10]

4.2.3 Orthopyroxene

Orthopyroxenes ($Wo_{0.8-1.0}En_{91}Fs_{7.2}$) have 2% Al_2O_3 and Cr_2O_3 levels ranging from ~0.3 to 0.8% (Table 3). Figure 2 [10] with the compositions of Mg-enstatite (Mg# = 90.6 - 92.4; $En_{88.7-89.}4Wo_{1.2-1.5}Fs_{10.1-9.1}$) have been analyzed in the lherzolite xenoliths from Hosséré Tello. These values are similar to those calculated for the lherzolite xenoliths from Spinel-lherzolite xenoliths from the Aritain Volcano, NE-Jordan [12] and significant works on the mantle xenoliths sampled along the Cameroon Volcanic Line. The X_{Mg} value varies in the same range as olivine.

4.2.4 Spinel

Spinel crystals display homogenous compositions with Mg# and Cr# ranging from 81.1 to 81.9 and from 10.6 to 10.8 respectively (Figure 4). The average composition of spinel as listed in Table 4 is close to $Mg_{0.7}sFe^{2+}_{0.22}Al_{1.65}Cr_{0.33}$ $Fe^{2+}_{0.0204}$. The X_{Mg} value varies from 0.80 to 0.81 and the X_{Cr} value from 0.13 to 0. 14. Al and Cr are relatively reversed correlated to each other. TiO_2 contents are low (~0.10 wt%)

Table 2. Clinopyroxene compositions (wt% and a.p.f.u. on the basis of 6 oxygens)

Data /Point	132 /	133 /	135 /	148 /	149 /	150 /	151 /	146 /	154 /	155 /
SiO_2	53.20	53.15	53.09	52.72	52.64	53.30	53.40	53.38	53.74	53.40
TiO_2	0.28	0.28	0.26	0.25	0.27	0.30	0.25	0.21	0.17	0.21
Al_2O_3	4.48	4.37	4.29	4.30	4.36	4.49	4.64	4.28	4.39	4.47
Cr_2O_3	1.56	1.56	1.43	1.48	1.57	1.55	1.66	1.44	1.41	1.61
FeO	2.03	1.94	2.10	2.13	2.21	2.02	1.91	2.18	1.96	1.85
MnO	0.10	0.06	0.07	0.03	0.07	0.06	0.08	0.05	0.10	0.06
MgO	15.88	15.79	15.96	16.01	15.92	15.76	15.63	15.65	15.92	15.38
CaO	21.20	21.12	20.87	21.00	20.79	21.08	20.89	21.23	21.21	21.08
Na_2O	0.05	0.06	0.03	0.03	0.00	0.05	0.06	0.01	0.06	0.06
K_2O	1.71	1.80	1.80	1.65	1.60	1.83	1.69	1.68	1.73	1.82
Total	100.49	100.13	99.90	99.64	99.42	100.45	100.26	100.14	100.71	99.95
Wo(Ca)	1.89	2.00	2.26	2.23	1.67	1.91	0.47	1.23	1.43	0.88
En (Mg)	0.33	0.13	0.07	0.12	0.70	0.30	1.49	1.07	0.67	1.06
Fs($Fe^{2+}Fe^{3+}$Mn)	100.68	100.33	100.12	99.86	99.59	100.63	100.31	100.27	100.85	100.03
Si	1.924	1.929	1.931	1.924	1.924	1.928	1.932	1.937	1.936	1.939
Al^{iv}	0.076	0.071	0.069	0.076	0.076	0.072	0.068	0.063	0.064	0.061
Al^{vi}	0.115	0.116	0.114	0.109	0.112	0.120	0.130	0.120	0.123	0.130
Al^T	0.191	0.187	0.184	0.185	0.188	0.192	0.198	0.183	0.186	0.191
Ti	0.008	0.008	0.007	0.007	0.007	0.008	0.007	0.006	0.005	0.006
Cr	0.045	0.045	0.041	0.043	0.045	0.044	0.048	0.041	0.040	0.046
Fe^{3+}	0.000	0.000	0.000	0.000	0.000	0.000	0.000	0.000	0.000	0.000
Fe^{2+}	0.061	0.059	0.064	0.065	0.067	0.061	0.058	0.066	0.059	0.056
Mn	0.003	0.002	0.002	0.001	0.002	0.002	0.002	0.002	0.003	0.002
Mg	0.856	0.854	0.865	0.871	0.867	0.850	0.843	0.846	0.855	0.833
Ca	0.821	0.821	0.813	0.821	0.814	0.817	0.810	0.825	0.819	0.820
Na	0.004	0.004	0.002	0.002	0.000	0.003	0.004	0.001	0.004	0.004
Mg#	0.93	0.94	0.93	0.93	0.93	0.93	0.94	0.93	0.94	0.94

Table 3. Orthopyroxene compositions (wt% and a.p.f.u. on the basis of oxygens).

Data /Point	130 /1.	131 /1.	136 / 1.	137 / 1.	138/1	141 /1	157 /1.	147 /1.	152 /1.	153 / 1.
SiO_2	56.61	56.75	57.21	57.06	56.68	57.21	56.66	56.78	56.98	56.72
TiO_2	0.06	0.08	0.12	0.06	0.04	0.00	0.07	0.04	0.08	0.05
Al_2O_3	2.56	2.35	2.34	2.38	2.45	2.42	2.32	2.57	2.32	2.34
Cr_2O_3	0.50	0.40	0.42	0.48	0.43	0.45	0.43	0.51	0.45	0.42
FeO	5.03	4.89	5.05	5.09	4.94	4.92	4.98	4.97	4.91	4.89
MnO	0.10	0.14	0.16	0.11	0.11	0.11	0.16	0.11	0.09	0.08
MgO	34.56	34.99	34.86	34.71	34.43	34.93	34.92	34.86	34.60	35.17
CaO	0.60	0.59	0.50	0.69	0.65	0.49	0.55	0.65	0.49	0.58
Na_2O	0.09	0.09	0.10	0.08	0.07	0.12	0.08	0.08	0.08	0.10
Total	100.11	100.28	100.78	100.66	99.81	100.65	100.17	100.58	99.99	100.34
Si	1.929	1.939	1.948	1.946	1.948	1.949	1.939	1.936	1.953	1.935
Al^{iv}	0.071	0.061	0.052	0.054	0.052	0.051	0.061	0.064	0.047	0.065
Al^{vi}	0.033	0.033	0.042	0.042	0.047	0.046	0.033	0.039	0.046	0.029
Ti	0.001	0.002	0.003	0.002	0.001	0.000	0.002	0.001	0.002	0.001
Cr	0.014	0.011	0.011	0.013	0.012	0.012	0.012	0.014	0.012	0.011
Fe^{3+}	0.030	0.020	0.000	0.002	0.000	0.001	0.020	0.014	0.000	0.028
Fe^{2+}	0.115	0.120	0.144	0.143	0.142	0.139	0.123	0.128	0.141	0.112
Mn	0.003	0.004	0.005	0.003	0.003	0.003	0.004	0.003	0.003	0.002
Mg	1.774	1.782	1.770	1.765	1.764	1.774	1.781	1.772	1.768	1.789
Ca	0.022	0.022	0.018	0.025	0.024	0.018	0.020	0.024	0.018	0.021
Na	0.006	0.006	0.007	0.006	0.005	0.008	0.006	0.005	0.005	0.006
K	0.002	0.000	0.000	0.000	0.000	0.000	0.000	0.000	0.001	0.000
Wo (Ca)	1.14	1.11	0.95	1.30	1.24	0.92	1.04	1.22	0.93	1.08
En (Mg)	91.26	91.51	91.38	91.05	91.23	91.68	91.42	91.30	91.64	91.66
Fs($Fe^{2+}Fe^{3+}$Mn)	7.60	7.38	7.67	7.65	7.52	7.40	7.55	7.48	7.43	7.26

Table 4. Spinel compositions (wt% and a.p.f.u. on the basis of 32 oxygens).

Data/Point	128 /1	129 / 1	144 / 1	145 / 1
SiO_2	0.02	0.36	0.00	0.06
TiO_2	0.18	0.21	0.14	0.17
Al_2O_3	34.64	34.91	35.13	35.01
Cr_2O_3	32.81	32.67	32.86	33.16
FeO	13.04	13.21	12.94	12.96
MnO	0.12	0.15	0.17	0.12
MgO	17.55	17.34	17.95	17.46
CaO	0.00	0.00	0.00	0.00
Na_2O	0.00	0.00	0.00	0.00
NiO	0.20	0.24	0.21	0.24
P_2O_5	0.00	0.00	0.02	0.00
Total	98.59	99.11	99.41	99.17
Fe_2O_3 (calc)	3.23	2.38	3.50	2.70
FeO (calc)	10.14	11.06	9.79	10.53
Total (calc)	98.90	99.34	99.76	99.44
Si	0.01	0.08	0.00	0.01
Ti	0.03	0.04	0.02	0.03

Table 4 continued

Data/Point	128 /1	129 / 1	144 / 1	145 / 1
Al	9.40	9.43	9.43	9.45
Cr	5.97	5.92	5.92	6.00
Fe^{3+}	0.56	0.41	0.60	0.46
Fe^{2+}	1.95	2.12	1.86	2.02
Mn	0.02	0.03	0.03	0.02
Mg	6.02	5.92	6.09	5.96
Ca	0.00	0.00	0.00	0.00
Na	0.00	0.00	0.00	0.00
Ni	0.04	0.04	0.04	0.04
Cr#	0.39	0.39	0.39	0.39

and those of Al_2O_3 are high (up to 55 wt%). The Cr_2O_3 contents vary between 12.93 wt% and 13.45 wt% (Table 4).

4.2.5 Characterization of Xenoliths Studied According to Their Areas of Genesis

The Al^{VI}/Al^{IV} ratio, variable between 0.70 and 1.14, is similar to that of the clinopyroxenes of the peridotites of the subcontinental upper mantle of Ngaoundéré [13] and of the sublithospheric crust [14]. The diagram in Figure 4 below, shows the distribution of the different samples in two categories of cpx; the cpx domain of the lithospheric mantle and those of the lower crust. The samples from Tello, Likok and Ganguiré fall within the cpx domain of the lithospheric mantle [14], while those of Liri, Maz 1 and 2 fall within the cpx domain of the lower crust. According to the diagram in Figure 4 below, the Al^{IV} and Al^{VI} contents vary by 0.05-0.2 and 0.03-0.2 respectively. No sample falls into the granulitic xenolith facies domain, nor into the eclogite and igneous domain facies.

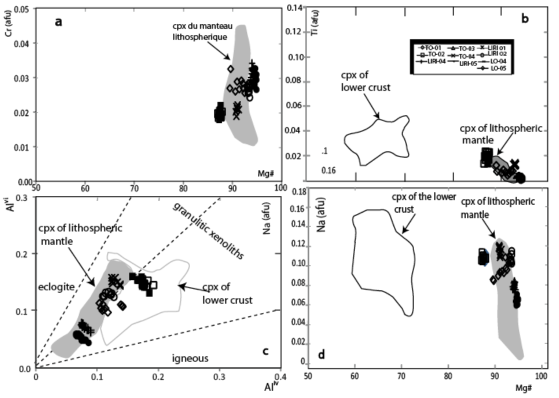

Figure 4. Variation of Cr (afu)versus Mg# (a), Al^{VI} versus Al^{IV} (c) , Ti (afu) and Na (afu)versus Mg# (=100*Fe^{2+}/ Fe^{2+}+Mg) (b and d), samples of lherzolite xenoliths fall within majority the scope of lithospheric mantle [14].

4.2.6 Spinel-Bearing lherzolite Xenoliths Origin

It is well known that spinel cannot be considered a single site ideal solution for Fe-Mg substitution due to interactions between X and Y sites, called reciprocal effects. The interactions of the cations (Al. Cr) in the Y sites of the spinel with the cations (Fe. Mg) in the X sites can be described by the following reaction:

$$FeAl_2O_4 + MgCr_2O_4 = FeCr_2O_4 + MgAl_2O_4 \text{ [15]}$$

Since spinel is a mineral rich in Cr compared to the other phases in which Cr is almost in trace, the ratio (Cr / Cr + Al) sp reflects that of the system and control (Mg / Mg + Fe^{2+}) sp. Autocorrelation is observed in Figure 5**.** This figure, which shows the reciprocal nature of the spinel solution, also illustrates a significant variation in (Cr / Cr + Al) of the system.

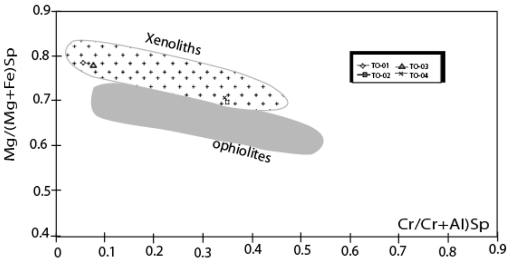

Figure 5. Mg # -Cr # autocorrelation diagram for the spinel phase. The ophiolite reference is reported after [16] a) Domain of ultrabasic enclaves (Lherzolites and Harburgites) in basic lavas b) Domain of ultrabasic rocks in ophiolites [16].

A well-defined domain can be clearly seen for the xenoliths studied which is placed above that corresponding to the ophiolitic massifs ophiolites field after [17]. This is the normal position of spinel peridotites typical of a lithospheric mantle sampled by alkaline magma soaked in a few hours. This characteristic leads us to believe that these peridotites are not portions of an ultrabasic body (tectonic scale) in the continental crust but that they have a deep origin in the mantle. This observation is quite similar with that of other xenoliths in the alkaline basalts of Cameroon [18]. The difference between the position of xenoliths and ophiolites has been explained by the kinetics of this exchange reaction. The refractory elements as Cr are enriched in the residue, as demonstrated for the Cr-rich clinopyroxene from Hosséré Addi xenoliths. Thus the studied spinel-bearing lherzolite xenoliths characterized by the presence of Cr-diopside represent probably portions of the upper mantle. However, the compositions of olivine and spinelle are highly dependent on the degree of fusion characterized by near constant values of (Mg#)Ol, (Mg#)Sp and (Cr#)Sp. On the basis of these data, Hosséré Tello xenoliths represent a residual sequence resulting from the partial fusion of a mantellic source. Experiments have shown that the composition of solid solutions such as olivine, is very sensitive to temperature changes and its constituents could evolve to refractory elements during partial fusion. So an extraction of the melt could leave a residue depleted in highly incompatible elements (e.g. Na. Al. K. and Ti) and enriched in Cr and Ni relative to the most primitive mantle. The range of Ni contents of olivine of lherzolites from Hosséré Tello confirms that they are residues of melting. The high Ni (2500 ppm - 4100 ppm) levels in olivine suggest that Hosséré Tello xenoliths may have originated from a low degree of fusion (~30%) from a relatively homogeneous mantellic source.Thus, the model for portions of the earth's upper mantle appears appropriate for the origin of the Hosséré Addi spinel-bearing lherzolite xenoliths.

5. Geochemestry and Geothermobarometry

5.1 The Rare Earths Elements of the Clinopyroxenes of the Samples from Tello

There are significant depletions of zirconium, titanium, and yttrium relative to elements with similar compatibilities (REE) (Table 5). Rare earth spectra differ slightly. In the Tello sector, two scenarios are clearly distinguished (Figure 6). The first characterizes clinopyroxenes with LaN enrichment relative to chondrites and nearly equal Ce, Pr Nd contents. This reflects the presence of a concavity within the light rare earths. The spectrum of clinopyroxenes at the medium rare earth level is almost linear, reflecting the same Sm, Eu and Gd contents. A slight depletion of heavy earths is also observed. The second scenario is characterized by increasing pace from La to Lu marking a slight enrichment in heavy and almost rectilinear rare earths.

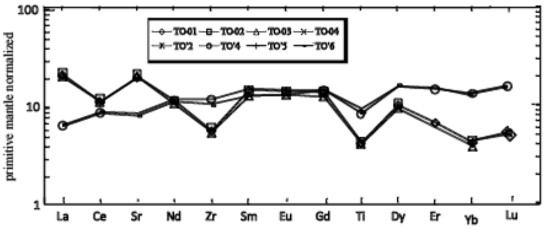

Figure 6. Primitive mantle normalized REE patterns in Clinopyroxene from Tello peridotite xenoliths

5.2 Comparison between the Trace Elements of Clinopyroxenes of Tello and Other Sectors

Compared to rare earths elements, the trace elements in clinopyroxene are almost similar. Weak anomalies in Ba, Nb and Ti and a strong negative anomaly in Pb are observed in all the samples of the xenoliths (Figure 7, Table 5). The general shape of the spectra follows the same contours except for a slight difference observed at the level of the Tello xenoliths. The spectra on the whole are therefore homogeneous. Pb depletion in cpx is a function of mobilization by metasomatic fluids. In fact, it is the character that explains the compatibility of lead with the metalliferous deposits of the continental crust where fluids play a primordial role [19] after a partial melting of the mantle.

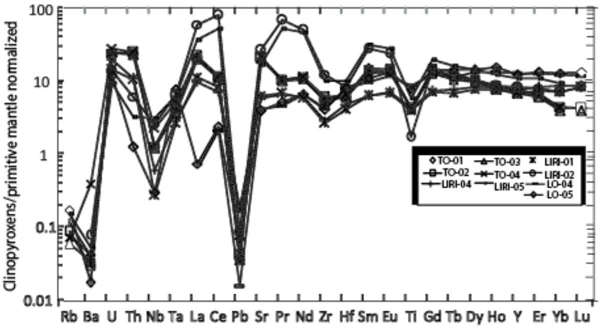

Figure 7. Multi-element spectra of clinopyroxene from the peridotites of the 03 previously stated localities and Tello peridotites, normalized to the values of the primitive mantle (Sun and Mc Donough, 1989)

5.3 Geothermobarometry

The use of Bertrand and Mercier thermometers (1985), T (B&M), and that of Brey and Köhler (1990), T (B&K), is based on exchanges between orthopyroxen-clinopyroxen [20]. An equilibrium temperature of approximately 905 °C was estimated for Hosséré Tello's lherzolite-spinel xenoliths [21]. Geothermometer (Table 6), based on the solubility of Al_2O_3 in orthopyroxen and spinel, the expression of the calibrated temperature at the pressure of 1.5 GPa in a natural spinel lherzolite system, gives the equilibrium temperatures of Hosséré Tello's lherzolite to spinel xenoliths from 1215 °C - 1245 °C. The Hosséré Addi (Tello) xenoliths were probably sampled by the host basalt of the upper sublithospheric mantle at depths of 25 km to 36 km, and calculated temperatures are about 200 °C above those of the oceanic geothermal. The maximum pressure can be calculated from the composition of the spinel [22] or established with the crystalline chemistry data of the clinopyroxene to determine the variability of the pressure during partial fusion.

Table 5. Chemical analyzes of rare earths and trace elements in the Cpx of the different localities

	TO-01	TO-02	TO-03	TO-04	TO’2	TO’4	TO’5	TO’6
La	20.963	21.900	19.898	20.750	6.216	6.374	5.539	6.574
Ce	11.174	11.870	11.008	11.157	8.455	8.654	7.875	8.803
Sr	19.779	21.103	20.023	21.249	7.973	8.504	7.368	7.882
Nd	11.516	11.384	10.610	11.096	10.986	11.782	10.787	11.671
Zr	5.596	6.020	5.332	5.878	10.485	11.873	10.914	10.198
Sm	14.616	14.412	12.712	13.528	12.508	14.956	11.693	14.616
Eu	14.214	14.071	13.000	13.411	12.839	14.536	13.071	14.071
Gd	13.795	14.079	12.497	13.545	14.446	14.496	13.123	14.547
Ti	4.201	4.254	4.114	4.248	9.268	8.438	8.589	8.716
Dy	10.301	10.630	9.559	9.971	15.657	15.904	13.679	16.605
Er	6.784	6.621	6.067	6.337	15.356	14.915	13.971	12.775
Yb	4.234	4.449	3.865	4.197	12.671	13.631	13.212	12.246
Lu	4.160	4.160	3.914	3.909	13.827	12.346	12.016	12.757

Table 6. geothermometric estimation (°C) of ultramafic xenoliths

Lherzolites	**Sample**		**Methode**		**Sample**		**Methode**	
		opx-sp	**Opx-ca**			**opx-sp**	**Opx-ca**	
		B&M	**B&K1**	**B&K2**		**B&M**	**B&K1**	**B&K2**
Samples	**TO$_3$**		834.27	892.11	**TO$_1$**	1187.69	984.24	933.41
			849.61	890.10		1117.02	919.86	927.75
			869.38	900.89		1119.39	911.48	894.46
			846.00	880.45			936.28	962.11
			848.87	894.07		1140.33	915.78	950.96
			852.36	924.89			921.03	889.01
			849.19	910.34			932.31	914.09
			852.11	919.68			970.39	947.81
			856.53	904.37			911.62	890.00
			834.30	902.60			934.81	922.66
			831.01	885.53			954.98	910.35
			851.31	891.39			936.56	920.89
			854.96	869.21				
	TO$_2$	1103.93	865.29	852.13				
		1112.43	844.68	874.37				
		1101.90	846.02	865.10				
			856.41	898.59				
			824.67	864.47				
			843.25	874.08				

The xenoliths of the mantle of Hosséré Tello as for most of the xenoliths of the Cameroon Line show that they are peridotites of lherzolithe to spinel, not containing plagioclase or garnet and are derived from the spinel stability field in the mantle which is in a pressure range of ~ 0.8 GPa to ~2 GPa [22,23]. These estimated pressures may be associated with depths of 30 km to 60 km as reported for the other Lherzolite spinel [24,25].

6. Discussion and Conclusions

Considering the investigations of trace elements in single grain, clinopyroxenes provide reliable information about chemical composition. The trace elements composition of clinopyroxene analyzed in spinel-lherzolite xenoliths from Tello is therefore a useful indicator of chemical modification in the mantle. According to Jankovics et al. [14], the samples from Tello, fall within the cpx domain of the lithospheric mantle. According to the diagram in Figure 4, the Al^{iv} and Al^{vi} contents vary by 0.05-0.2 and 0.03-0.2 respectively. No sample falls into the granulitic xenolith facies domain, nor into the eclogite and igneous domain facies. The spinel peridotites typical of a lithospheric mantle is sampled by alkaline magma soaked in a few hours. Thus, Figure 4 allows the studied spinel-bearing lherzolite xenoliths characterized by the presence of Cr-diopside which represent probably portions of the upper mantle [14]. We observe in all the samples of the xenoliths the weak anomalies in Ba, Nb and Ti and a strong negative anomaly in Pb (Figure 6).

The slight depletion of rare earths elements in the analyzed clinopyroxenes (Tello 01, Tello 02, Tello 04, Tello 4) compared with the other REE observed in the others clinopyroxenes from Tello is indicative of a partial melting episode. Our results are similar to those described by Nkouandou et al. [26], that the general shape of the spectra follows the same contours except for a slight difference observed at the level of the Tello xenoliths. The spectra on the whole are therefore homogeneous. Pb depletion in cpx is a function of mobilization by metasomatic fluids. In fact, it is the character that explains the compatibility of lead with the metalliferous deposits of the continental crust where fluids play a primordial role [14]. The compositions of their silicate minerals are typical of equilibrated Mg-rich olivine. Al-rich enstatite and Cr-diopside in the upper mantle. Similar compositions have been recorded in minerals of ultramafic xenoliths from other ultramafic xenoliths domains of the Cameroon Volcanic Line and the Adamawa Plateau. Thus, ultramafic xenoliths from Hosséré Addi represent peridotites sampled from lithospheric mantle and hosted in the basaltic lava flowed. The spinel-bearing lherzolite xenoliths show internal chemical homogeneity and their mineral chemistries suggest equilibrium conditions of 820 °C-1200 °C.

Conflict of Interest

There is no conflict of interest.

References

[1] Déruelle, B., Ngounouno, I., Demaiffe, D., 2007 The "Cameroon Hot Line" (CHL): A unique example of active alkaline intraplate structure in both oceanic and continental lithospheres. C.R. Geos. 339, 589-600.

[2] Kamgang, P., 2003. Pétrologie et géochimie d'un secteur clé de la Ligne du Cameroun, les monts Bamenda: Implications sur la genèse et l'évolution des magmas. Thèse Doct. D'Etatn Univ. Ydé. I. pp. 373.

[3] Fitton, J.G., Dunlop, H.M., 1985. The Cameroon line, West Africa, and its bearing on the origin of oceanic and continental alcali basalt. Earth Planet Sci let. 72, 23-38.

[4] Tchoua, M.F., 1974. Contribution à l'étude géologique et pétrologique de quelques volcans de la "Ligne du Cameroun" (Monts Manengouba et Bambouto). Thèse Doct. d'Etat. Univ. Clérmont-Ferrand. pp. 337.

[5] Dumont, J.F., Toteu, S.F., 1984. Sur deux cycles de migmatisation dans la zone mobile panafricaine, au Nord Cameroun, 10 R.A.S.T., Bordeaux.

[6] Tchameni, R., Pouclet, A., Penaye, J., et al., 2006. Petrography and Geochemistry of the Ngaoundéré Pan-African Granitoids in Central North Cameroon: Implications for Their Sources and Geological Setting. Journal of African Earth Sciences. 44, 511-529. DOI: http://dx.doi.org/10.1016/j.jafrearsci.2005.11.017

[7] Le Maréchal, A., 1976. Géologie et géochimie des sources thermo-minérales du Cameroun. *Travaux et documents ORSTROM, Paris.* 59, 1-175.

[8] Mercier, J.C., Nicolas, A., 1975. Textures and fabrics of upper mantle peridotites as illustrated by xenoliths from basalts. Jour Petrol. 16, 454-487.

[9] Kretz, R., 1983. Symbols for rock-forming minerals. Amer Miner. 68, 277-279.

[10] Morimoto, N., 1989. Nomenclature of Pyroxenes. Canadian Mineralogist. 27, 143-154.

[11] Dal Negro, A., Carbonin, S., Domeneghetti, C., et al., 1984. Crystal Chemistry and Evolution of the Clinopyroxene in a Suite of High Pressure Ultramafic Nodules from the Newer Volcanics of Victoria. Australia. Contributions to Mineralogy and Petrology. 86, 221-229.

[12] Nasir, S., A1-Fuqha, H., 1988. Spinel-Lherzolite Xenoliths from the Aritain Volcano. NE-Jordan.

[13] Dautria, J.M., Girod, M., 1986. Les enclaves de lherzolite à spinelle et plagioclase du volcan de Dibi (Adamaoua, Cameroun): des témoins du manteau anormal. Bulletin De Mineralogie. 109, 275-286.

[14] Jankovics, É., Dobosi, G., Embey-Isztin, A., et al., 2013. Origin and ascent history of unusually crystal-rich alkaline basaltic magmas from the western Pannonian Basin. Bulletin Volcanol. 75(749), 1-23.

[15] Matsui, Y., Nishizawa, O., 1974. Iron (II) - magnesium exchange equilibrium between olivine and calcium-free over a temperature range 800°C to 1300°C. Bulletin de la Société française de Minéralogie et de Cristallographie. 97, 122-130.

[16] Green, D.H., Hibberson, W., 1970. The Instability of Plagioclase in Peridotite at High Pressure. Lithos. 3,

209-221.
DOI: http://dx.doi.org/10.1016/0024-4937(70)90074-5

[17] Gasparik, T., 1987. Orthopyroxene Thermobarometry in Simple and Complex Systems. Contributions to Mineralogy and Petrology. 96, 357-370.
DOI: http://dx.doi.org/10.1007/BF00371254

[18] O'reilly, S.Y., Chen, D., Griffin, W., et al., 1997. Minor Elements in Olivine from Spinel Lherzolite Xenoliths: Implications for Thermobarometry. Mineralogical Magazine. 61, 257-269.
DOI: http://dx.doi.org/10.1180/minmag.1997.061.405.09

[19] Zindler, A., Hart, S.R., 1986. Chemical geodynamics. Annual Review of Earth and Planetary Sciences. 14, 493-571.

[20] Bertrand, P., Sotin, C., Gaulier, J.M., et al., 1987. La solubilité de l'aluminium dans l'orthopyroxène globale des données expérimentales du systeme MgO-Al_2O_3-SiO_2. Bulletin de la Societé Géologique de France. 8, 821-832.

[21] O'neill, H.S.C., 1981. The Transition between Spinel Lherzolite and Garnet Lherzolite.

[22] Clark Jr., S.J., Ringwood, A.E., 1964. Density Distribution and Constitution of the Mantle. Reviews of Geophysics. 2, 35-88.
DOI: http://dx.doi.org/10.1029/RG002i001p00035

[23] Lee, D.C., Halliday, A.N., Davies, G.R., et al., 1996. Melt Enrichment of Shallow Depleted Mantle: A Detailed Petrological. Trace Element and Isotopic Study of Mantle-Derived Xenoliths and Megacrysts from the Cameroon Line. Journal of Petrology. 37, 415-441.
DOI: http://dx.doi.org/10.1016/j.crte.2007.10.012

[24] Green, D.H., Ringwood, A.E., 1967. The Genesis of Basaltic Magmas. Contributions to Mineralogy and Petrology. 15, 103-190.
DOI: http://dx.doi.org/10.1007/BF00372052

[25] Mysen, B.O., Kushiro, I., 1977. Compositional Variations of Coexisting Phases with Degrees of Melting of Peridotte in the Upper Mantle. American Mineralogist. 62, 843-865.

[26] Nkouandou, O.F., Temdjim, R., 2011. Petrology of Spinel Lherzolite Xenoliths and Host Basaltic Lava from Ngao Voglar Volcano. Adamawa Massif (Cameroon Volcanic Line. West Africa): Equilibrium Conditions and Mantle Characteristics. Journal of Geosciences. 56, 375-387.